

DOI: 10.1002/zaac.202200167

# Synthesis and properties of a new vanadium benzene-1,3-diphosphonate

Felix Steinke<sup>[a]</sup> and Norbert Stock<sup>\*[a, b]</sup>

Dedication to Professor Dr. Wolfgang Schnick on the occasion of his 65th birthday

The use of the linker molecule benzene-1,3-diphosphonic acid ( $H_4L$ ) and  $V^{4+}$ -ions in a hydrothermal synthesis without further additives led to the discovery of a new coordination polymer of composition  $[(VO)_2(H_2O)_4(L)] \cdot 2H_2O$ . The structure of the compound was solved by direct methods from powder X-ray

diffraction data and refined using the Rietveld method. The compound was thoroughly characterized showing a reversible amorphization upon reduced pressure or high temperatures. A potential porosity was calculated, but could not be verified by  $H_2O$ -adsorption experiments.

## Introduction

Metal-organic frameworks (MOFs) have been intensively investigated in the last decades.<sup>[1]</sup> There are several examples in which the use of relatively simple linker molecules such as terephthalic or isophthalic acid resulted in highly porous compounds with a variety of structures and properties e.g. MOF-5,<sup>[2]</sup> MIL-53,<sup>[3]</sup> UiO-66<sup>[4]</sup> or CAU-10.<sup>[5]</sup> The use of the phosphonate-based analogues on the other hand are far less studied. This is due to the limited commercial availability and the tendency of metal phosphonates to form layered non-porous compounds.<sup>[6]</sup> Hence over the last years the use of sterically demanding tri- and tetraphosphonic acids as linker molecules was intensively investigated and highly porous metal phosphonates could be obtained.<sup>[7]</sup> However, the use of diphosphonic acids remains an area of interest. For the linker molecule benzene-1,4-diphosphonate, the CSD (Nov. 21) lists 100 crystal structures in the MOF subset,<sup>[1]</sup> while the carboxylate analogue terephthalate was reported in 4131 crystal structures. The use of the V-shaped benzene-1,3-diphosphonic acid (Figure 1) resulted in only 18 crystalline compounds also clearly outnumbered by the metal isophthalates (1878 entries). Addi-

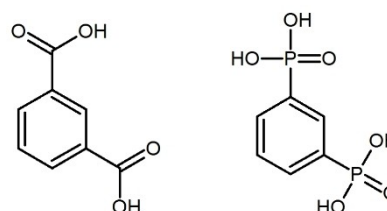


**Figure 1.** Isophthalic acid (left) and the phosphonic acid analogue benzene-1,3-diphosphonic acid ( $H_4L$ ). Both V-shaped linker molecules were reported for the synthesis of MOFs and coordination polymers. While 1878 metal isophthalates have been reported, only 18 metal benzene-1,3-diphosphonates are known (CSD, 11.2021).

tionally, for the reported crystal structures containing benzene-1,3-diphosphonate only metal ions of uranium, copper and vanadium are known (Table S1).<sup>[8,9,10,11]</sup> For the five reported vanadium-based compounds exclusively  $V^{5+}$  salts were used as starting material, and in one case the reduction of  $V^{5+}$  into  $V^{4+}$  and the formation of vanadyl ions ( $VO^{2+}$ ) during the solvothermal synthesis was observed.<sup>[10]</sup>

Herein we report the synthesis of the new vanadyl phosphonate  $[(VO)_2(H_2O)_4(L)]$  ( $L^{4-}$  = benzene-1,3-diphosphonate) starting from  $VO_4$ . The structure was fully resolved from powder X-ray diffraction (PXRD) data. Phase purity was confirmed by thermogravimetric measurements (TG) and elemental analyses. Based on the structural data a potential  $H_2O$  accessible surface area of  $770 \text{ m}^2/\text{g}$  and a limiting pore diameter of  $2.97 \text{ \AA}$  was calculated but no suitable activation conditions could be found, to confirm porosity by  $H_2O$  sorption measurements.

## Results and Discussion

### Synthesis

The linker molecule benzene-1,3-diphosphonic acid ( $H_4L$ ) was synthesized within 21 hours at  $170^\circ\text{C}$  under an  $N_2$  atmosphere

[a] F. Steinke, Prof. Dr. N. Stock  
Institute of Inorganic Chemistry  
Christian-Albrechts-Universität zu Kiel  
Max-Eyth-Str. 2, 24118 Kiel,  
Germany  
E-mail: stock@ac.uni-kiel.de

[b] Prof. Dr. N. Stock  
Kiel Nano, Surface and Interface Science KiNSIS,  
Kiel University, Christian-Albrechts-Platz 4,  
D-24118 Kiel, Germany

Supporting information for this article is available on the WWW under <https://doi.org/10.1002/zaac.202200167>

© 2022 The Authors. Zeitschrift für anorganische und allgemeine Chemie published by Wiley-VCH GmbH. This is an open access article under the terms of the Creative Commons Attribution License, which permits use, distribution and reproduction in any medium, provided the original work is properly cited.

starting from 1,3-dibromobenzene and using a nickel catalyst as reported for the syntheses of other phosphonic acids.<sup>[8,10,12]</sup> A syringe-pump was used to ensure slow and continuous addition of the triethylphosphite without poisoning of the nickel catalyst. The successful C–P coupling was confirmed by <sup>1</sup>H- and <sup>31</sup>P-NMR spectroscopy (Figure S1). The hydrolysis of the phosphonate ester was accomplished by refluxing the ester in hydrochloric acid. The vanadium phosphonate [(VO)<sub>2</sub>(H<sub>2</sub>O)<sub>4</sub>(L)]·2H<sub>2</sub>O was hydrothermally synthesized as a microcrystalline, phase-pure product within 2 days at 160 °C using the linker, VOSO<sub>4</sub> and water as solvent. It was first obtained at a 1 mL scale and the process was successfully scaled up by a factor of 10. Detailed descriptions are given in the *Experimental* section.

### Crystal structure determination

A powder X-ray diffraction pattern of [(VO)<sub>2</sub>(H<sub>2</sub>O)<sub>4</sub>(L)]·2H<sub>2</sub>O was successfully indexed in a tetragonal unit cell and the extinction conditions point at the space group *I*4<sub>1</sub>/*acd* (Nr. 142) using Topas Academics.<sup>[13]</sup> The structure was solved in the lower symmetry space group *I*4<sub>1</sub>/*a*, employing direct methods as implemented in EXPO2014,<sup>[14]</sup> which led to the localisation of the heavy atoms (vanadium and phosphorous) and atomic positions that could be assigned to a distorted benzene ring. The structure was completed using the software Materials Studio<sup>[15]</sup> and force field calculations were applied to geometrically optimize the structure. The symmetry of the crystal structure was transformed into the space group *I*4<sub>1</sub>/*acd* using the software Vesta.<sup>[16]</sup> Finally, the crystal structure was refined using the Rietveld-algorithm<sup>[17]</sup> as implemented in Topas Academics.<sup>[13]</sup> For the refinement, sets of distance and angle restraints for the C–C, C–P and P–O bonds were employed. Electron density located in pores was accounted as oxygen atoms representing water as guest molecules. One guest per asymmetric unit was refined on a general position without restraints. The final results of the Rietveld refinement are shown in Figure 2 and a good agreement between the calculated and the observed PXRD pattern is found. The crystallographic data of [(VO)<sub>2</sub>(H<sub>2</sub>O)<sub>4</sub>(L)]·2H<sub>2</sub>O is shown in Table 1.

### Structure description

While a detailed structure discussion for [(VO)<sub>2</sub>(H<sub>2</sub>O)<sub>4</sub>(L)]·2H<sub>2</sub>O is given in the SI, only significant parts of the structure are described here. The refined bond lengths and angles are in good agreement with data of other vanadyl phosphonates listed in the CSD, which were analysed using the software Conquest and Mercury.<sup>[18]</sup> The asymmetric unit of the title compound is shown in Figure 3b. The vanadyl-ion was identified by the shortest V–O bond distance of 1.601(12) Å. The coordinating water molecules on the other hand exhibit larger V–O distances of 2.365(11) Å and 2.169(12) Å. The V–O distances to the phosphonate groups range from 1.925(13) to

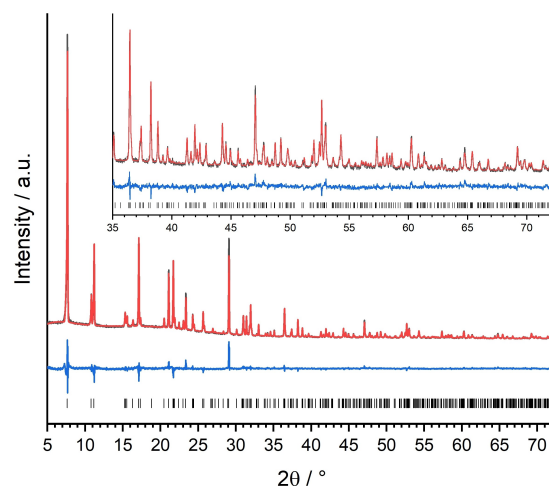


**Figure 2.** Final Rietveld-plot of the structure refinement of [(VO)<sub>2</sub>(H<sub>2</sub>O)<sub>4</sub>(L)]·2H<sub>2</sub>O. The measured X-ray powder diffractogram (black line), the calculated diffractogram (red), the resulting difference (blue) and the allowed reflection positions (black ticks) are shown.

**Table 1.** Crystallographic data of the title compound.

parameter	[(VO) <sub>2</sub> (H <sub>2</sub> O) <sub>4</sub> (L)]·2H <sub>2</sub> O
space group	<i>I</i> 4 <sub>1</sub> / <i>acd</i>
<i>a</i> , <i>b</i> /Å	23.2069(3)
<i>c</i> /Å	12.29130(17)
Volume/Å <sup>3</sup>	6619.66(17)
R <sub>wp</sub> /%	6.46
GoF/%	2.33
R <sub>Bragg</sub> /%	3.96

2.018(15) Å (Table S2). The vanadium ions are surrounded by six oxygen atoms (Figure 3a).

Each linker molecule coordinates with all oxygen atoms to six isolated vanadyl-moieties (Figure 3c) along the 4<sub>1</sub>-screw axis resulting in a rod shaped inorganic building unit (IBU) composed of alternating CPO<sub>3</sub> and VO<sub>6</sub> polyhedra along the *c* axis (Figure 3d). Linker molecules interconnect the IBUs to four other IBUs in the *a*,*b* plane (Figure 3e), so the structure of [(VO)<sub>2</sub>(H<sub>2</sub>O)<sub>4</sub>(L)]·2H<sub>2</sub>O can be described as a 1<sup>0</sup>O<sup>2</sup> coordination network.<sup>[19]</sup> Based on donor-acceptor-distances, hydrogen bonds between neighbouring IBUs are postulated. The observed distances between the vanadyl-oxygen atom and the opposite water ligand (O4–O6) is 2.774(17) Å and therefore in the range of medium-strong hydrogen bonds (Figure S2).<sup>[20]</sup>

A topological analysis of the crystal structure following a standard simplification with vanadium and phosphorous atoms as nodes results in a new 2-nodal 3,4-*c* net with the extended point symbol  $\{4.6.8\}\{4.6^2.8^3\}$  (Figure 3f). Channel-type, helical micropores are found along [001]. A limiting pore diameter of 2.97 Å was calculated using PoreBlazer<sup>[21]</sup> after adding hydrogen atoms to the linker moieties using EXPO2014.<sup>[14]</sup>

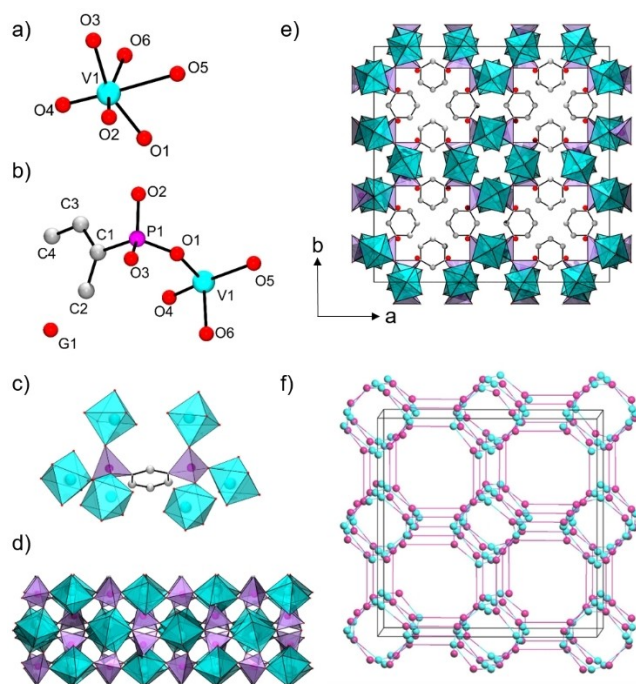


**Figure 3.** a) Coordination environment of the vanadium ions in the title compound. b) Asymmetric unit in the structure of the title compound. c) Bridging of six  $\text{VO}_6$ -moieties by one linker molecule. d) IBU of the title compound as seen along [100]. e) Structure of the title compound as seen along [001]. f) Simplified 3,4-c net of the structure of the title compound. General color scheme:  $\text{VO}_6$  = blue,  $\text{CPO}_3$  = violet, O = red, C = grey.

### Thermal properties

Thermal properties were determined by thermogravimetric (TG) and variable temperature (VT-) PXRD measurements (Figure 4, Figures S4, S5). The thermogravimetric measurement shows the

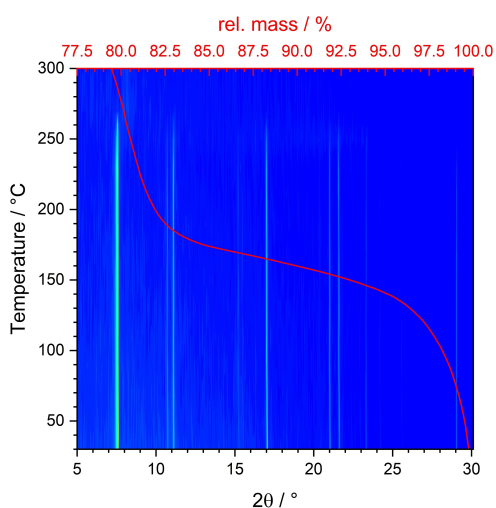


**Figure 4.** TG data combined with VT-PXRD patterns of  $[(\text{VO})_2(\text{H}_2\text{O})_4(\text{L})] \cdot 2\text{H}_2\text{O}$  between room temperature and 300 °C.

expected loss of five water molecules between room temperature and 200 °C (obs. 19.6%, calc. 18.9%), followed by the additional loss of one coordinated water molecule (obs. 3.8% calc. 3.8%) per formula unit. The linker molecule starts to decompose between 500 and 600 °C and an X-ray amorphous glass is formed.

According to the VT-PXRD study (Figure 4), up to 250 °C only small changes in the diffraction patterns are observed which are due to the loss of  $\text{H}_2\text{O}$  and to thermal effects. The crystallinity of  $[(\text{VO})_2(\text{H}_2\text{O})_4(\text{L})] \cdot 2\text{H}_2\text{O}$  is lost at temperatures above 260 °C.

A sequential refinement of the lattice parameters (details are given in the SI, Figure S6 and Table S8) allow to get an insight into the structural changes. Only a minor increase in the lattice parameters  $a$  and  $b$  is found while  $c$  only decreases just before the loss of crystallinity. A slight decrease in the cell volume is observed in the temperature range between 100 and 150 °C, which can be explained by the desorption of water molecules from the structure. However, the total increase of the unit cell volume between RT and 250 °C is below 1%. The crystal structure decomposes at temperatures above 260 °C as can be seen in the VT-PXRD data, while thermal decomposition of the linker molecule is observed in the TG data at much higher temperatures. Since the VT-PXRD data shows, that the framework is stable up to 250 °C it should be possible to remove some of the water molecules from the coordination environment of the vanadium without destroying the structure. It is noted, that results of VT-PXRD and TG measurements can differ since the former are carried out in open capillaries while the latter were done in a constant air stream. Thus some differences in the decomposition temperatures are found.

### Sorption measurements

The potential porosity of  $[(\text{VO})_2(\text{H}_2\text{O})_4(\text{L})] \cdot 2\text{H}_2\text{O}$  was proven *in silico* using the software suites PoreBlazer,<sup>[21]</sup> Zeo++<sup>[22]</sup> and Materials Studio.<sup>[15]</sup> Only micropores with a limiting pore diameter of 2.97 Å are present and therefore  $\text{N}_2$  adsorption ( $d_{\text{kin}} = 3.6$  Å) at 77 K is not expected. In contrast, water adsorption ( $d_{\text{kin}} = 2.6$  Å) at 298 K is anticipated. Figure 5 shows the solvent accessible surface area (770  $\text{m}^2/\text{g}$ ) calculated for water molecules.

However, a  $\text{H}_2\text{O}$ -uptake was not observed in adsorption measurements after testing different activation conditions. Procedures, which involved elevated temperatures (80–200 °C) with or without reduced pressure, resulted in the loss of long-range order of the compound which is accompanied by a color change from bright blue to black (Figure 6 and Figures S7 and S8). Crystallinity was reestablished by stirring the activated samples in  $\text{H}_2\text{O}$  for 16 hours (Figure 6). Removal of all coordinating water molecules at temperatures above 260 °C lead to irreversible structural changes, which is in line with the results from the VT-PXRD study.

Using an even milder activation procedure involving a partial solvent exchange with MeOH prior to the sorption measurement and applying reduced pressure at room temper-

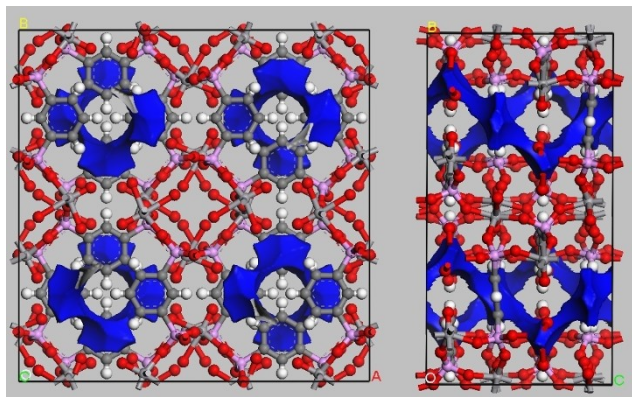


**Figure 5.** Solvent accessible surface areas (blue) calculated for water molecules ( $d_{\text{kin}} = 2.6 \text{ \AA}$ ) as seen along [001] (left) and [100] (right). The protons of the linker molecules were added using EXPO2014<sup>[14]</sup> and the surface area was calculated using Zeo++<sup>[22]</sup> and visualized using Materials Studio.<sup>[15]</sup>

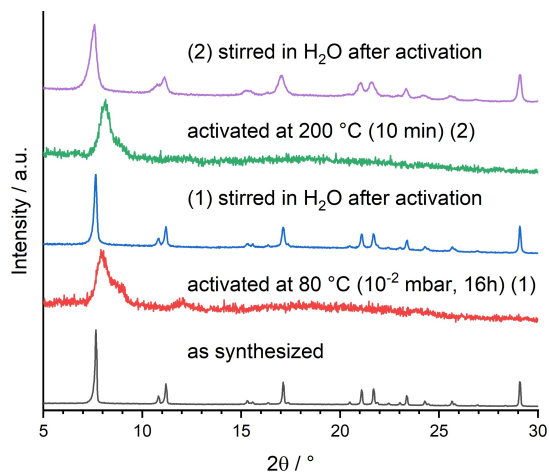


**Figure 6.** PXRD patterns of  $[(\text{VO})_2(\text{H}_2\text{O})_4(\text{L})] \cdot 2\text{H}_2\text{O}$ . Black: The as synthesized compound; Red: The sample activated at  $80^\circ\text{C}$  under reduced pressure ( $p < 10^{-2}$  mbar) (1); Blue: The activated sample (1) stirred in  $\text{H}_2\text{O}$  for 16 hours; Green: The sample activated at  $200^\circ\text{C}$  (2); Violet: The activated sample (2) stirred in  $\text{H}_2\text{O}$ .

ature, did not lead to the loss of long-range order but only a very small  $\text{H}_2\text{O}$ -uptake of 3.1 wgt% or 0.86 mol/mol was found for this sample (Figure S9). Thus the milder activation conditions lead only to a partial removal of the guest molecules, maintaining the crystallinity, while harsher conditions result in the loss of long range order and loss of porosity.

### IR spectroscopy

IR spectroscopy was used to further characterize  $[(\text{VO})_2(\text{H}_2\text{O})_4(\text{L})] \cdot 2\text{H}_2\text{O}$ . An assignment of the most prominent bands is given in the SI (Table S4). Most of the observed bands (Figure S10) are caused by vibrations of the linker molecules. Thus, the bands around  $1500$  and  $1600 \text{ cm}^{-1}$  correspond to

aromatic in plane stretching vibrations of the phenyl-rings. In addition, the absorption bands around  $1150\text{--}1023 \text{ cm}^{-1}$  correspond to the P–O stretching vibration of the phosphonate groups. The bands between  $3578$  and  $3330 \text{ cm}^{-1}$  can be assigned to the OH-valence vibration of coordinating water involved in hydrogen bonding.<sup>[23]</sup>

### Conclusions

In conclusion, we presented the synthesis and characterization of a new microcrystalline vanadium phosphonate. The structure of the title compound was solved *ab initio* from PXRD data using direct methods and refined using the Rietveld algorithm. TG and VT-PXRD measurements demonstrated a thermal stability up to  $250^\circ\text{C}$ , while various activation procedures led to a loss of long range order at lower temperatures accompanied by a notable change of color. Crystallinity of the activated compounds is accomplished by stirring the sample in  $\text{H}_2\text{O}$  at room temperature.

A potential porosity of the compound was calculated *in silico* but  $\text{H}_2\text{O}$  adsorption experiments did not confirm the expected  $\text{H}_2\text{O}$  uptake.

### Experimental Section

#### Materials and methods

All starting materials and solvents were used without further purification.  $\text{VOSO}_4 \cdot 5\text{H}_2\text{O}$  was purchased from Alfa Aesar,  $\text{NiCl}_2$  from Fluka, 1,3-diisopropylbenzene and 1,3-dibromobenzene from Sigma. Hydrochloric acid (37%) from VWR chemical was used. PXRD patterns were collected on a STOE Stadi P-Combi and on a STOE Stadi MP instrument equipped both with a MYTHEN 1 K detector and using  $\text{Cu-K}\alpha_1$  radiation. MIR-spectra were collected using a BrukerALPHA-FT-IR A220/D-01 with an ATR-unit.  $^1\text{H}$  and  $^{31}\text{P}$ -NMR spectra were recorded with a Bruker AVANCE III HD Pulse Fourier Transform spectrometer equipped with a cryo-probehead Prodigy BBO400S1 BB-H&F-D-05-Z operating at a frequencies of  $400.13 \text{ MHz}$  ( $^1\text{H}$ ) or  $161.98 \text{ MHz}$  ( $^{31}\text{P}$ ). Prior to the measurement the sample was dissolved in a solution of  $\text{NaOD}$  in  $\text{D}_2\text{O}$  (10%). The elemental analyses were conducted employing a vario MICRO cube Elementaranalysator from Elementar. Thermogravimetric data was collected on a Linseis STA PT 1600 (airflow =  $6 \text{ L/h}$ , heating rate =  $4 \text{ Kmin}^{-1}$ ). Sorption measurements were carried out using a BEL Japan Inc. BELSORP-max with water vapour at  $298 \text{ K}$ . The samples were treated for 10 minutes or 16 h at a temperature of  $25/80/200^\circ\text{C}$ , respectively, under reduced pressure ( $p < 10^{-2}$  mbar) or nitrogen flow prior to the measurements. The syntheses of the title compounds were carried out in a Memmert UNB 500 oven with forced ventilation and a programmable temperature-time-program using custom-made steel autoclaves with Teflon® inserts (total volume of  $2 \text{ ml}$  and  $20 \text{ mL}$ ).<sup>[24]</sup> Variable temperature PXRD data (VT-PXRD) was collected with a Stoe capillary furnace in  $0.5 \text{ mm}$  quartz capillaries. The temperature range between  $30$  and  $300^\circ\text{C}$  was studied and the sample was heated in steps of  $20^\circ\text{C}$ .

## Synthesis of the linker molecule benzene-1,3-diphosphonic acid

The linker molecule was obtained, following a two-step synthesis similar to published routines.<sup>[11]</sup> First, 1,3-dibromobenzene (1.967 g, 1.008 mL, 8.34 mmol) together with anhydrous NiCl<sub>2</sub> (0.72 g, 5.55 mmol) was stirred in 56 mL 1,3-diisopropylbenzene at 170 °C under an N<sub>2</sub>-atmosphere. Employing a syringe pump, triethylphosphite (6.00 mL, 34.8 mmol) was added within one hour. Afterwards, the mixture was kept for 20 hours at 170 °C. After cooling to room temperature, the catalyst was separated from the mixture by vacuum filtration. The solvent was removed by evaporation under reduced pressure and the obtained liquid was dissolved in 20 mL dichloromethane and washed with water (3 × 40 mL). The solvent of the organic phase was removed by rotary evaporation and 1,3-bis(diethylphosphono)-benzene was obtained as an orange oil, which was treated under reflux in 50 mL concentrated hydrochloric acid (37%) for 16 hours. After removal of the hydrochloric acid and ethanol under reduced pressure the obtained waxy solid was stirred two times in 100 mL diethyl ether for 2 h to remove impurities from the hydrolysis and improve crystallinity. After vacuum filtration, benzene-1,3-diphosphonic acid was obtained as an off-white powder (1.02 g, 4.29 mmol, 51.4% based on 1,3-dibromobenzene).

<sup>1</sup>H-NMR (400 MHz, NaOD in D<sub>2</sub>O (10%)): δ = 7.51 (t, 1H, J = 11.6 Hz), 7.27 (m, 2H), 6.98 (m, 1H) ppm.

<sup>31</sup>P-NMR (162 MHz, NaOD in D<sub>2</sub>O (10%)): δ = 12.01 (s, 2P) ppm.

## Synthesis of [(VO)<sub>2</sub>(H<sub>2</sub>O)<sub>4</sub>(L)] · 2H<sub>2</sub>O

The title compound was first synthesized by introducing 11.9 mg (0.05 mmol) benzene-1,3-diphosphonic acid, 900 μL H<sub>2</sub>O and 100 μL of an aqueous solution of VOSO<sub>4</sub> (c = 1 mol/L, 0.1 mmol) into a Teflon reactor. The reactor, placed in a custom-made steel multiclave and heated to 160 °C during 6 hours, kept at 160 °C for 24 hours and finally cooled to room temperature within 6 hours. [(VO)<sub>2</sub>(H<sub>2</sub>O)<sub>4</sub>(L)] · 2H<sub>2</sub>O was obtained as a bright blue powder after filtration and washing with 5 mL H<sub>2</sub>O and MeOH respectively. For further characterisation, a synthesis scale-up was carried out using 10-fold amounts. 119 mg (0.5 mmol) benzene-1,3-diphosphonic acid, 9 mL H<sub>2</sub>O were placed in a 30 mL Teflon reactor. 1 mL of an aqueous VOSO<sub>4</sub> solution (c = 1 mol/L, 1 mmol) was added and the Teflon reactor was closed and placed in a steel autoclave. Using a conventional oven, the reactor was heated to 160 °C using the same temperature-time-program as described before. The product was obtained through vacuum filtration, washed with 20 mL H<sub>2</sub>O and MeOH respectively and dried at air. [(VO)<sub>2</sub>(H<sub>2</sub>O)<sub>4</sub>(L)] · 2H<sub>2</sub>O was obtained as a bright blue powder (192.2 mg, 87.4%).

Elemental analysis of the title compound [(VO)<sub>2</sub>(H<sub>2</sub>O)<sub>4</sub>(C<sub>6</sub>H<sub>4</sub>P<sub>2</sub>O<sub>6</sub>)] · 2H<sub>2</sub>O (measured/calculated): C = 15.8/15.1 %, H = 3.57/3.39 %.

## Acknowledgements

Financial support by the state of Schleswig-Holstein is acknowledged. The authors thank Mirjam Poschmann, Bastian Achenbach, Jonas Gosch, as well as the spectroscopic section of the Institute of Inorganic Chemistry of Kiel University for their support with various measurements. Open Access funding enabled and organized by Projekt DEAL.

## Conflict of Interest

The authors declare no conflict of interest.

## Data Availability Statement

The data that support the findings of this study are available from the corresponding author upon reasonable request.

**Keywords:** vanadium phosphonate · metal-organic framework · Rietveld refinement · hydrothermal synthesis · powder X-ray diffraction

- [1] P. Z. Moghadam, A. Li, S. B. Wiggin, A. Tao, A. G. P. Maloney, P. A. Wood, S. C. Ward, D. Fairen-Jimenez, *Chem. Mater.* **2017**, *29*, 2618–2625.
- [2] H. Li, M. Eddaoudi, M. O’Keeffe, O. M. Yaghi, *Nature* **1999**, *402*, 276–279.
- [3] T. Loiseau, C. Serre, C. Huguenard, G. Fink, F. Taulelle, M. Henry, T. Bataille, G. Férey, *Chemistry* **2004**, *10*, 1373–1382.
- [4] J. H. Cavka, S. Jakobsen, U. Olsbye, N. Guillou, C. Lamberti, S. Bordiga, K. P. Lillerud, *J. Am. Chem. Soc.* **2008**, *130*, 13850–13851.
- [5] H. Reinsch, M. A. van der Veen, B. Gil, B. Marszalek, T. Verbiest, D. de Vos, N. Stock, *Chem. Mater.* **2013**, *25*, 17–26.
- [6] a) F. Steinke, N. Stock, *Z. Anorg. Allg. Chem.* **2021**, *112*, 1034; b) F. Costantino, P. L. Gentili, N. Audebrand, *Inorg. Chem. Commun.* **2009**, *12*, 406–408; c) H. P. Perry, K. J. Gagnon, J. Law, S. Teat, A. Clearfield, *Dalton Trans.* **2012**, *41*, 3985–3994; d) A. Clearfield, *Chem. Mater.* **1998**, *10*, 2801–2810.
- [7] a) N. Hermer, H. Reinsch, P. Mayer, N. Stock, *CrystEngComm* **2016**, *18*, 8147–8150; b) M. Taddei, F. Costantino, F. Marmottini, A. Comotti, P. Sozzani, R. Vivani, *Chem. Commun.* **2014**, *50*, 14831–14834; c) T. Rhauderwiek, K. Wolkersdörfer, S. Øien-Ødegaard, K.-P. Lillerud, M. Wark, N. Stock, *Chem. Commun.* **2018**, *54*, 389–392; d) T. Zheng, Z. Yang, D. Gui, Z. Liu, X. Wang, X. Dai, S. Liu, L. Zhang, Y. Gao, L. Chen, D. Sheng, Y. Wang, J. Diwu, J. Wang, R. Zhou, Z. Chai, T. E. Albrecht-Schmitt, S. Wang, *Nat. Commun.* **2017**, *8*, 15369; e) S. Wöhlbrandt, C. Meier, H. Reinsch, E. Svensson Grape, A. K. Inge, N. Stock, *Inorg. Chem.* **2020**, *59*, 13343–13352.
- [8] P. DeBurgomaster, W. Ouellette, H. Liu, C. J. O’Connor, J. Zubietta, *CrystEngComm* **2010**, *12*, 446–469.
- [9] a) P. DeBurgomaster, J. Zubietta, *Acta Crystallogr. Sect. E* **2010**, *66*, m1304–m1305; b) Y. Wang, X. Wang, D. Zhang, F. Zhou, D. Gui, T. Zheng, J. Li, Z. Chai, S. Wang, *CrystEngComm* **2018**, *20*, 3153–3157; c) Y. Wang, D. Zeng, F. Zhou, D. Zhang, J. Li, T. Zheng, *J. Mol. Struct.* **2018**, *1173*, 183–187; d) T. Zheng, Y. Gao, D. Gui, L. Chen, D. Sheng, J. Diwu, Z. Chai, T. E. Albrecht-Schmitt, S. Wang, *Dalton Trans.* **2016**, *45*, 9031–9035.
- [10] W. Ouellette, G. Wang, H. Liu, G. T. Yee, C. J. O’Connor, J. Zubietta, *Inorg. Chem.* **2009**, *48*, 953–963.
- [11] T. Zheng, Y. Gao, L. Chen, Z. Liu, J. Diwu, Z. Chai, T. E. Albrecht-Schmitt, S. Wang, *Dalton Trans.* **2015**, *44*, 18158–18166.
- [12] F. Steinke, A. Javed, S. Wöhlbrandt, M. Tiemann, N. Stock, *Dalton Trans.* **2021**, *50*, 13572–13579.
- [13] A. A. Coelho, *J. Appl. Crystallogr.* **2018**, *51*, 210–218.
- [14] A. Altomare, C. Cuocci, C. Giacovazzo, A. Moliterni, R. Rizzi, N. Corriero, A. Falcicchio, *J. Appl. Crystallogr.* **2013**, *46*, 1231–1235.
- [15] Accelrys Incorporated, *Materials Studio*, San Diego, **2009**.
- [16] K. Momma, F. Izumi, *J. Appl. Crystallogr.* **2011**, *44*, 1272–1276.
- [17] H. M. Rietveld, *Acta Crystallogr.* **1967**, *22*, 151–152.

- [18] I. J. Bruno, J. C. Cole, P. R. Edgington, M. Kessler, C. F. Macrae, P. McCabe, J. Pearson, R. Taylor, *Acta Crystallogr. Sect. B* **2002**, *58*, 389–397.
- [19] A. K. Cheetham, C. N. R. Rao, R. K. Feller, *Chem. Commun.* **2006**, 4780–4795.
- [20] G. A. Jeffrey, in *An introduction to hydrogen bonding*, Oxford Univ. Press, New York, **1997**.
- [21] L. Sarkisov, R. Bueno-Perez, M. Sutharson, D. Fairen-Jimenez, *Chem. Mater.* **2020**, *32*, 9849–9867.
- [22] T. F. Willems, C. H. Rycroft, M. Kazi, J. C. Meza, M. Haranczyk, *Microporous Mesoporous Mater.* **2012**, *149*, 134–141.
- [23] G. Socrates, in *Infrared and Raman characteristic group frequencies. Tables and charts*, Wiley, Chichester, **2001**.
- [24] N. Stock, T. Bein, *Angew. Chem. Int. Ed. Engl.* **2004**, *43*, 749–752.

---

Manuscript received: May 5, 2022

Revised manuscript received: June 9, 2022